

Supplementary Materials

LanEvil: Benchmarking the Robustness of Lane Detection to Environmental Illusions

Anonymous Author(s)

Submission Id: 1807

A MORE DETAILS OF *LANEVIL* DATASET

In this section, we delve into more details of the *LanEvil* dataset design, covering severity design, a comparison of relevant studies, and visualization.

A.1 Illusion Design Details

Here, we offer a comprehensive introduction to the designs encompassing five distinct severity levels across various illusion types.

Road Crack. For the Road Crack illusion, we incorporate circular network cracks and bar-shaped cracks onto the road surface. These cracks, colored black, vary in size (*i.e.*, diameter or length) from 0.5m to 5m and appear multiple times along a 30m long path. Following the definition in Section 3.2, we represent the number of applied cracks as N_{crack} . For the five severity levels, we set N_{crack} as $\{3, 5, 10, 20, 30\}$ from level-1 to level-5.

Road Repair. Similar to Road Crack, we employ facilities such as manhole covers, sewer outlets, and road joint tape. These facilities appear multiple times within a 30m range, with types randomly selected, and lengths ranging from 0.3m to 3m, determined by the real-world characteristics of the corresponding objects. We use N_{repair} to denote the number of applied facilities. For Road Repair illusion type, all disturbances are achieved by modifying the appearance, and we set the N_{repair} as $\{1, 3, 5, 10, 15\}$.

Tire Marks. For Tire Marks, we add one pair of tire prints. There are two types of tire prints: straight and curved, with lengths ranging from 3m to 10m. To denote varying levels of severity, we regulate the degree of clarity by adjusting the center distance between the tire prints and the road surface in the simulation environment. The closer the distance, the more distinct the Tire Marks become. We express the distance between these two facilities as a percentage of the height of the tire prints: $\{40\%, 30\%, 20\%, 10\%, 0\%\}$.

Guard Rail. Different from the first three illusion types, the modification method of Guard Rail is to add new facilities. We select various types of guard rails and place them in the environment, arranging them in a direction as parallel to the lane line as possible. The length of an individual guard rail facility is approximately 2m, so as the quantity increases, the overall length also expands. Specifically, let N_{guard} represent the number of Guard Rail. We set N_{guard} as $\{5, 10, 15, 20, 25\}$.

Pedestrian. In the dynamic objects illusion category, we utilize automatic generation and navigation methods. Specifically, we select objects corresponding to a specific type (*e.g.*, Pedestrian) and generate them at randomly chosen spawn points. Subsequently, we assign speeds to different objects and activate automatic control. For Pedestrian, we set the number of generated pedestrians as $\{25, 50, 75, 100, 125\}$.

Vehicle. For Vehicle, we set the number of generated vehicles as $\{50, 75, 100, 125, 150\}$. It is worth noting that, the types of

Vehicle and Bicycle in CARLA are stored in the same assets *vehicle*. We manually distinguish the models of two types.

Bicycle. For Bicycle, we set the number of generated bicycles as $\{20, 40, 60, 80, 100\}$. It is worth noting that our focus is not solely on bicycles (human-powered), but we include all two-wheeled vehicles in this illusion type.

Streetlight. We adjust the angle of sunlight, denoted as a , to create different streetlight shadows. Specifically, we ensure that the shadow length crosses the current lane, generating streetlight shadows with angles of approximately $\{60^\circ, 55^\circ, 50^\circ, 45^\circ, 40^\circ\}$ relative to the lane line. The smaller the angle, the greater the amplitude of the illusion.

Fence. We manually construct a continuous arrangement of fences and adjust the angle of sunlight to create densely packed shadows on the road surface. Specifically, we generate shadows with different tilt angles $\{60^\circ, 55^\circ, 50^\circ, 45^\circ, 40^\circ\}$ similar to streetlights.

Rail. Different from the previous two illusion types, the rails are usually built diagonally above the road. We generate shadows at different positions by fixing the azimuth of the sun while adjusting the sun's altitude and the height of the rails. The generated shadows are approximately $\{2.0, 1.5, 1.0, 0.5, 0\}$ meters away from the center of the current lane.

Wire. Wires are almost directly above the road surface, so we fix the azimuth of the sun and adjust the sun altitude to project their shadows onto the road surface similar to Rail. The shadows are $\{2.0, 1.5, 1.0, 0.5, 0\}$ meters away from the center of the current lane.

Sunlight/Streetlight Reflection. Reflection primarily occurs when there is water on the road surface. For Sunlight Reflection, we set various lower values for sun altitude, while for Streetlight Reflection, we choose two common light colors: white and yellow. We control the water volume variable to adjust severity levels. Specifically, we set water volume as $\{40.0, 50.0, 60.0, 70.0, 80.0\}$.

Vehicle Reflection. Unlike the previous one that used water to control the illusion, adjusting the light intensity l can control the reflection generated by the vehicle. Here we rely on fog to adjust the lighting intensity l . Thus, we set fog density relative to the clear atmosphere as $\{40\%, 30\%, 20\%, 10\%, 0\%\}$.

A.2 Comparison with Related Work

As discussed in Section 2.2, several LD datasets have been proposed. In this study, we conduct a comparison between our *LanEvil* dataset and eight classical datasets, focusing on scenario diversity and illusion categories. The detailed results are presented in Table 1. Our *LanEvil* dataset exhibits two distinctive characteristics. ① Our dataset covers various illusion categories. It's worth noting that while different illusions may appear in other datasets accidentally, they have not been distinguished in detail and lack sophisticated

design, limiting the possibility of conducting more in-depth research on them. ② Our dataset is designed to be “Editable”. This implies that customization is possible based on specific needs. In future open versions, we plan to release the scene files to the public, making our research more accessible and allowing others in the community to benefit from and build upon our work.

A.3 Visualization

We present the complete visualization of all 14 illusion types in Figure 1. Please note that the **red border** indicates the perturbed image containing the environmental illusion, while the black border indicates the original image used for comparison.

For additional visualizations and video results, please visit our website <https://lanevil.github.io/>.

B ADDITIONAL RESULTS ON COMMERCIAL SYSTEMS

B.1 OpenPilot Simulation

Table 2 shows the average ASR results of four illusion categories. When the Required Success Time is set to 2.50 seconds, the ASR of Road Crack, Shadow, and Reflection all exceeded 80%. Only the Traffic Obstruction category has a lower ASR of 21.58%. This is positive news for us, as Traffic Obstruction is a common occurrence on roads. Designers of autonomous vehicles should focus on mitigating the impact of these types of illusions on autonomous vehicle systems.

B.2 Apollo Simulation

We present experimental results utilizing Apollo for joint simulation, as illustrated in Figure 3. The vehicle can drive smoothly along the correct route in the original scene; while in the perturbed scene, once encountering the edge of the lane line, the vehicle stops moving. Quantitative results show that in the perturbed scene, the vehicle stops moving after driving for 2s without steering control. In the original scene, the vehicle’s turn control signal has already appeared at 1.5s, and the vehicle continues to drive for 15s until reaching the target point.

C LICENSE

The images in *LanEvil* dataset are released under the MIT License. For detailed provisions governing the use of the *LanEvil* dataset, please consult the official documentation at <https://mit-license.org/>.

D MORE DETAILS OF EXPERIMENT

D.1 Experimental Metrics

Accuracy. The detection Accuracy is defined as

$$Accuracy = \frac{\sum_{clip} C_{clip}}{\sum_{clip} S_{clip}}, \quad (1)$$

where C_{clip} and S_{clip} refer to the number of lane points predicted correctly and the number of total ground truth points respectively in the clip (or image). A lane point within 20 pixels the ground truth point is considered correct. Lane predictions are considered to be true positives (TP) only when more than 85% points are correct.

F1-score. We also employ F1-score defined as

$$F1 - score = \frac{2 \times Precision \times Recall}{Precision + Recall}, \quad (2)$$

where $Precision = \frac{TP}{TP+FP}$ and $Recall = \frac{TP}{TP+FN}$, corresponding the harmonic mean of precision and recall.

D.2 Main Results

For better analysis, we present the breakdown results of each illusion type in Accuracy and F1-score drop in Table 3, with detailed results placed at Section D.4.

① **Breakdown results analysis.** Similar to the results in Section 4.2, both metrics demonstrated a decrease in the majority of scenarios. However, there are also a few scenario indicators that remain essentially unchanged, and some even exhibit slight increases. This instructs the designers of the auto-drive system to prioritize attention to the more harmful illusion types.

② **Comparison of different backbones.** With the exception of SCNN models using only the VGG backbone, all other models based on the ResNet backbone show improved metrics with an increase in the number of model layers. However, while there is an overall performance improvement, the difference in metric decrease is not significant. This suggests that merely increasing the depth of the model may not be sufficient to effectively prevent environmental illusions.

③ **Comparison of different severity levels.** Figure 2 illustrates the Accuracy drop of various models using ResNet-18 backbone across different severity levels under 4 illusion categories. It is evident that as the severity level increases, the rate of decline in metrics shows a notable increase, particularly at level 5, where the model’s indicators can decrease by more than 30%.

D.3 More Details of Noise Defense Methods

D.3.1 Supplementary Explanation. In Figure 6 of the main text, we represent different illustration types using the numbers 1-14 due to space limitations. We clarify that their order corresponds to the sequence shown in Figure 1, where Road Crack is assigned the number 1 and Vehicle Reflection is assigned the number 14.

D.3.2 Implementation Details. **PGD adversarial training** [7]. The general process of adversarial training can be represented by the following min-max formula:

$$\min_{\theta} \mathbb{E}_{(I, \text{loc}_{gt}) \sim \mathcal{D}} \left[\max_{\|\delta\| \leq \epsilon} \mathcal{L}(f_{\theta}(I + \delta), \text{loc}_{gt}) \right], \quad (3)$$

where δ represents the tiny disturbance added to the input image and ϵ constrains the upper limit of the disturbance. PGD solves the maximization problem in the above equation through iterative attacks:

$$I_{t+1} = \prod_{I \pm \epsilon} (I_t + \alpha \cdot \text{sgn}(\nabla_I \mathcal{L}(f_{\theta}(I_t), \text{loc}_{gt}))). \quad (4)$$

In the PGD adversarial training process, we set ϵ to 0.02, α to 0.001, and the iterations are 30.

Cutout [3]. Cutout randomly masks out square regions of the input image during training to improve the robustness and generalization of CNN. We apply cutout on the training set of *LanEvil*

Table 1: Comparisons of *LanEvil* and other lane detection datasets. The “Size” column shows the number of images or frames for videos. The “Editable” column shows whether the dataset supports custom editing.

| Dataset | Year | Size | Editable | Scenario diversity | | | Illusion categories | | | |
|----------------|------|------------|----------|--|-----------|--|---|--|---|--|
| | | | | Scene type | Line type | Road type | Road Damage | Traffic Obstruction | Shadow | Reflection |
| CalTech [1] | 2008 | video 1224 | ✗ | urban | - | curve | - | vehicles | ordinary, few | sunlight, few |
| VPNet [6] | 2017 | image 20K | ✗ | urban | 8 | curve | - | vehicles | - | - |
| TuSimple [12] | 2017 | image 6408 | ✗ | highway | - | - | - | vehicles | - | - |
| CULane[8] | 2018 | image 133K | ✗ | urban, rural, highway | - | curve, crossroad | - | crowded road | ordinary, few | dazzle light, few |
| LLAMAS [2] | 2019 | image 100K | ✗ | highway | - | - | - | vehicles | - | - |
| BDD-100K [15] | 2020 | video 100K | ✗ | urban, highway, tunnel, residential | 11 | - | - | vehicles, persons, bikes, motors | - | - |
| CurveLane [14] | 2020 | image 150K | ✗ | urban, highway | - | 90% curve, S-curve, Y-lane | - | vehicles | - | - |
| VIL-100 [16] | 2021 | video 10K | ✗ | - | 10 | curve, crossroad | road damage, few | crowded road | ordinary, few | dazzle light, few |
| <i>LanEvil</i> | 2023 | image 90K | ✓ | urban, highway, rural, tunnel, residential | 9 | up/downhill, T-junction, crossroad, roundabout | road crack, road repair, tire marks, guard rail | vehicles, persons, bicycles, different traffic volumes | wire, fence, rail, streetlight subtly designed, challenging | strong sunlight, dazzy streetlight, puddle |

Table 2: Average ASR results under 8 chosen cases. 2.50s is the Required Success Time proposed by [10], and the corresponding columns in this table are bolded.

| Illusion Type | Required Success Time | | | | |
|---------------------|-----------------------|--------|--------|---------------|--------|
| | 1.75s | 2.00s | 2.25s | 2.50s | 2.75s |
| Road Crack | 89.74% | 87.18% | 89.74% | 92.31% | 92.61% |
| Traffic Obstruction | 18.95% | 19.47% | 21.05% | 21.58% | 22.63% |
| Shadow | 72.88% | 76.27% | 77.97% | 83.05% | 83.76% |
| Reflection | 79.50% | 80.23% | 81.91% | 83.60% | 84.32% |

during the data loading process. Specifically, we add a fixed 256 × 256 zero mask to a random location of each input image.

Copy-paste [5]. Copy-paste is a data augmentation method that copies a random subset of objects in one image and pastes them onto the other image, which is usually used in instance segmentation. In our experiments, we adopt similar ideas on the training set of *LanEvil*, but paste half of one image onto the other one, making it more suitable for lane detection. Specifically, for each target image (I_1), we randomly select one from the remaining images as the image to be copied (I_2). Then we randomly select a mask for the left or right half of the 1280 × 720 image and generate a new image by $I_1 \times (1 - \text{mask}) + I_2 \times \text{mask}$. Accordingly, we adjust the ground truth annotations by preserving the complete existing lane lines in two images and marking the removed part of lane lines as invisible manually.

Augment HSV. Augment HSV manipulates the Hue, Saturation and Value channels of an image to create new variations of the original data with different colors, brightness, and contrast. In our experiments, we set the range of HSV channel changes to the original -0.5 to 0.5. We perform the transformation on the HSV channel of the training set of *LanEvil* and then convert the HSV space images back to BGR format.

D.4 More Results

As mentioned in Section D.2, we present the original results of the experiment in this chapter. Table 4 displays the accuracy of all models in both the original and perturbed scenarios, while Table 5 presents the F1-score of all models in both the original and perturbed scenarios.

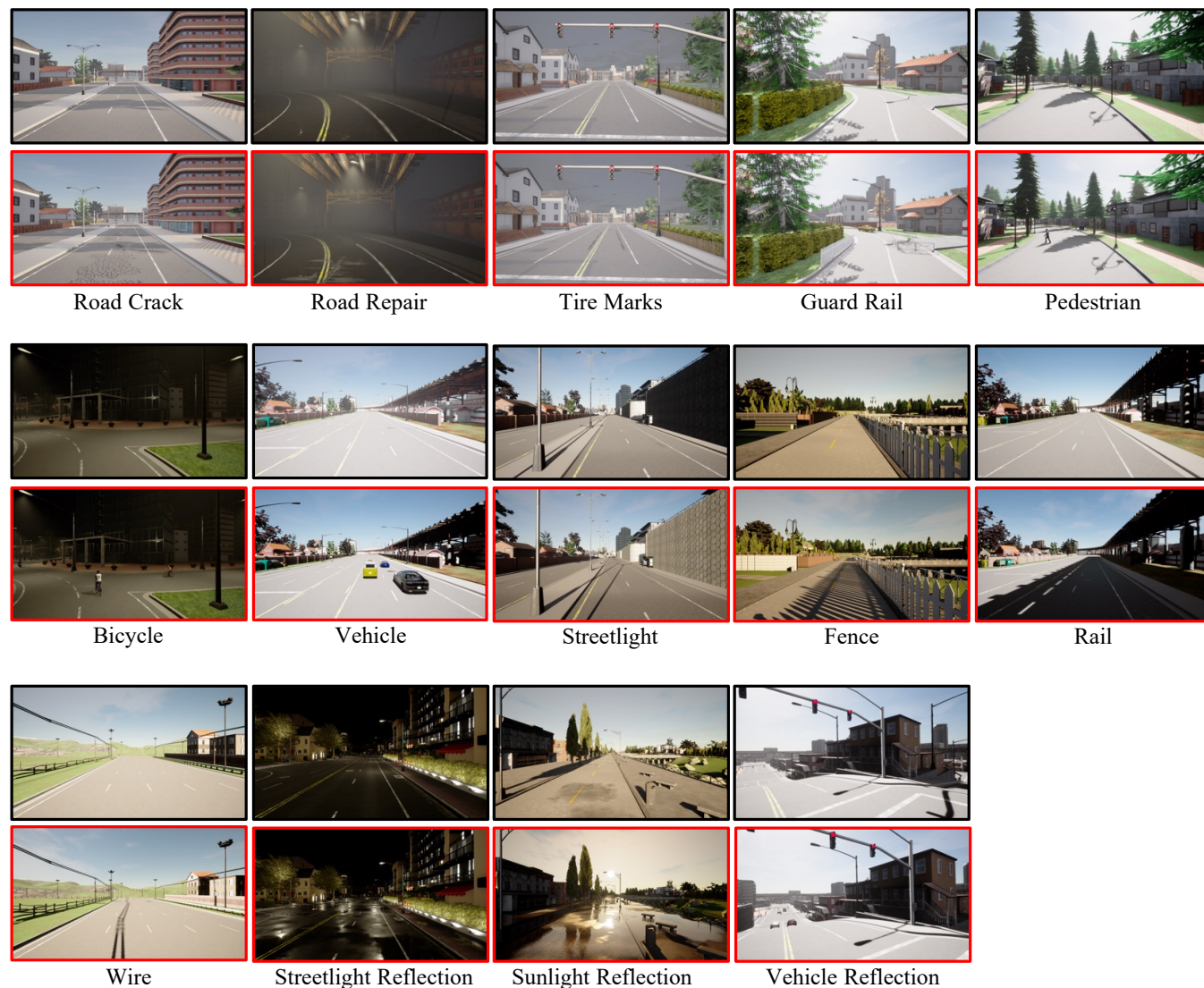


Figure 1: For each illusion type, we offer both the original and perturbed images. The original image is bordered in black, whereas the corrupted image is bordered in red.

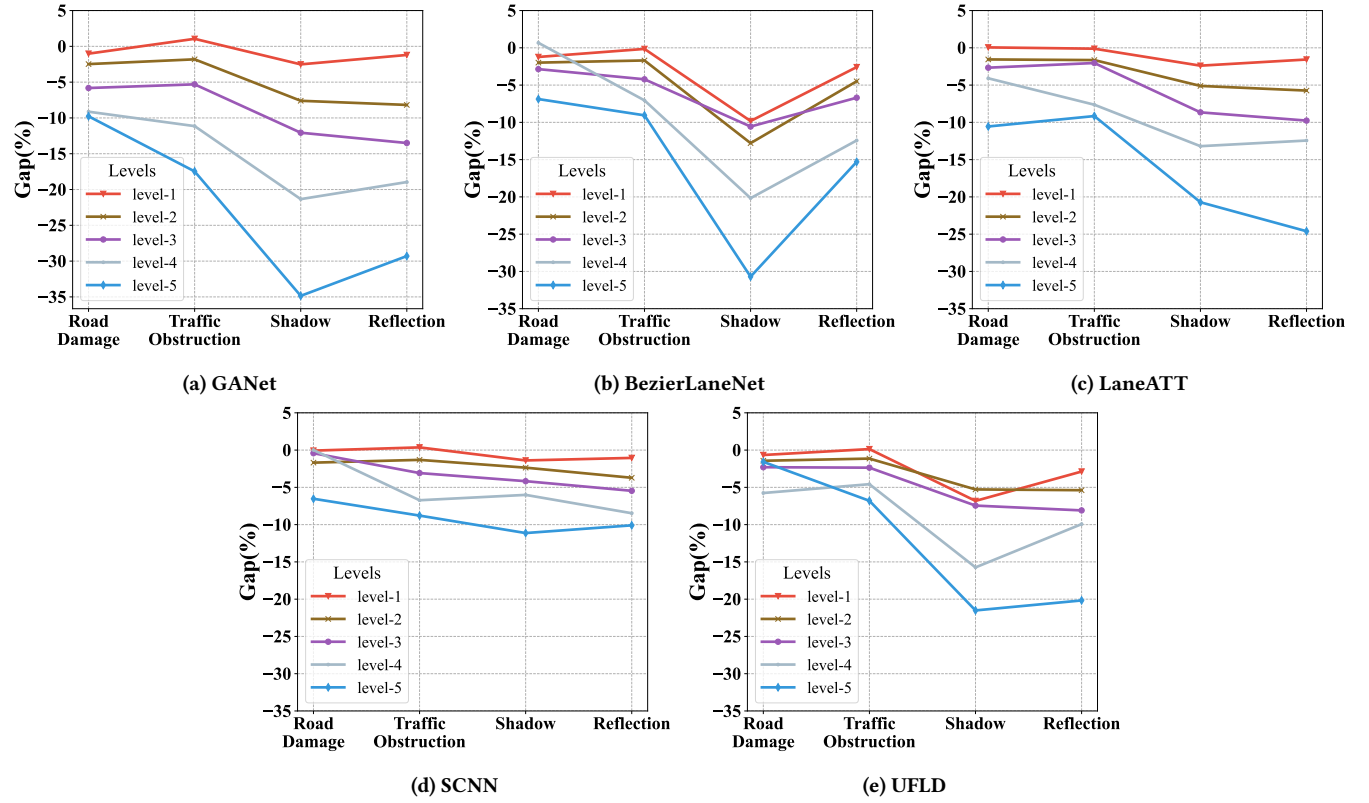


Figure 2: The Accuracy drop of various models using ResNet-18 backbone (SCNN uses VGG backbone) across different severity levels under 4 illusion categories.

Table 3: The breakdown results of each illusion type in Accuracy and F1-score drop (%).**(a) Results in Accuracy drop (%).**

| Method | Backbone | Road Damage | | | | Traffic Obstruction | | | Shadow | | | | Reflection | | |
|-------------------|----------|-------------|------------|-----------|-----------|---------------------|---------|------------|--------|-------|-------------|-------|-------------|----------|---------|
| | | RoadCrack | RoadRepair | TireMarks | GuardRail | Vehicle | Bicycle | Pedestrian | Fence | Rail | Streetlight | Wire | Streetlight | Sunlight | Vehicle |
| LaneATT [11] | Res-18 | -1.34 | -1.23 | -3.38 | -1.10 | -2.47 | -2.54 | -3.01 | -5.56 | -5.24 | -7.92 | -5.00 | -4.56 | -12.46 | 1.07 |
| | Res-34 | -0.14 | -1.39 | -2.77 | -0.30 | -2.32 | -1.98 | -0.12 | -2.01 | -0.91 | -1.70 | -4.67 | -5.08 | -0.63 | 0.00 |
| | Res-50 | -0.60 | -1.29 | -2.39 | -0.58 | -2.53 | -1.13 | -3.02 | -4.66 | -2.73 | -2.54 | -3.93 | -5.04 | -2.93 | 0.00 |
| | Res-101 | -0.10 | -0.49 | -2.31 | -0.42 | -1.22 | -1.11 | -3.07 | -3.93 | 0.09 | -2.98 | -0.15 | -3.40 | -3.06 | 0.00 |
| UFLD [9] | Res-18 | -0.48 | -1.90 | -4.89 | -0.22 | -2.60 | -1.66 | -1.47 | -7.12 | -6.75 | -5.71 | -6.87 | -4.87 | -10.74 | 2.01 |
| | Res-34 | -0.47 | -2.14 | -4.12 | -0.01 | -1.78 | -0.15 | -0.44 | -6.28 | -7.48 | -5.08 | -7.60 | -5.55 | -9.91 | -1.19 |
| | Res-50 | -0.54 | -1.57 | -2.63 | -0.06 | -2.30 | -1.87 | -0.64 | -7.96 | -6.23 | -6.52 | -2.51 | -3.84 | -7.53 | -1.34 |
| | Res-101 | -0.26 | -0.45 | -0.42 | -0.06 | -0.84 | -0.20 | -0.28 | -3.16 | -3.02 | -1.46 | -3.78 | -1.50 | -3.91 | -1.69 |
| BezierLaneNet [4] | Res-18 | -0.40 | -3.70 | -3.01 | -1.58 | -4.18 | -1.76 | -3.12 | -14.57 | -7.47 | -6.74 | -7.97 | -3.92 | -9.81 | 0.50 |
| | Res-34 | -0.21 | -0.03 | -2.75 | -0.55 | -3.35 | -0.22 | -2.66 | -4.67 | -8.55 | -6.98 | -2.46 | -4.51 | -0.22 | -0.42 |
| | Res-50 | -0.38 | -1.53 | -3.33 | -0.79 | -4.58 | -1.07 | -1.97 | -9.00 | -5.15 | -4.85 | -3.52 | -2.32 | -2.71 | -0.45 |
| | Res-101 | -0.10 | -3.66 | -1.93 | -0.91 | -0.79 | -1.47 | -1.76 | -11.50 | -2.23 | -2.14 | -1.80 | -2.05 | -2.82 | -0.10 |
| GANet [13] | Res-18 | -2.38 | -2.74 | -5.21 | -3.10 | -6.06 | -2.37 | -3.99 | -14.80 | -7.16 | -10.99 | -5.95 | -7.62 | -15.07 | 2.55 |
| | Res-34 | -0.41 | -2.33 | -0.53 | -3.11 | -1.21 | -0.06 | -0.62 | -12.77 | -3.57 | -0.13 | -6.22 | -8.72 | -0.38 | -1.58 |
| | Res-50 | -1.20 | -2.00 | -4.93 | -1.76 | -3.20 | -0.60 | -4.60 | -9.96 | -0.03 | -0.08 | -0.03 | -1.58 | -11.85 | -1.67 |
| | Res-101 | -0.56 | -1.24 | -2.21 | 0.02 | -1.07 | -2.47 | -2.28 | -2.64 | -0.25 | -0.82 | -2.18 | -2.36 | -2.18 | -1.84 |
| SCNN [8] | VGG | -3.10 | -0.01 | -0.53 | -1.53 | -3.14 | -1.69 | -2.61 | -4.73 | -4.56 | -5.69 | -2.39 | -2.87 | -6.65 | -0.92 |

(b) Results in F1-score drop (%).

| Method | Backbone | Road Damage | | | | Traffic Obstruction | | | Shadow | | | | Reflection | | |
|-------------------|----------|-------------|------------|-----------|-----------|---------------------|---------|------------|--------|--------|-------------|--------|-------------|----------|---------|
| | | RoadCrack | RoadRepair | TireMarks | GuardRail | Vehicle | Bicycle | Pedestrian | Fence | Rail | Streetlight | Wire | Streetlight | Sunlight | Vehicle |
| LaneATT [11] | Res-18 | -3.82 | -3.44 | -3.32 | -0.36 | -5.96 | -4.87 | -6.67 | -5.48 | -13.83 | -15.28 | -10.75 | -6.95 | -25.62 | 3.15 |
| | Res-34 | -3.16 | -3.65 | -1.77 | -0.37 | -6.40 | -3.62 | -3.06 | -2.07 | -7.50 | -11.16 | 0.05 | -2.00 | -0.77 | -0.01 |
| | Res-50 | -2.64 | -1.25 | -2.80 | -0.38 | -1.15 | -1.18 | -6.61 | -3.74 | -6.72 | -2.51 | 0.17 | -5.90 | -24.32 | -0.02 |
| | Res-101 | -2.63 | -0.60 | -1.64 | -0.27 | -2.64 | -5.68 | -1.25 | -4.78 | -8.31 | -6.80 | -10.22 | -5.26 | -24.83 | -0.01 |
| UFLD [9] | Res-18 | 1.16 | -1.20 | -7.00 | -0.20 | -5.00 | -3.07 | -2.63 | -8.27 | -12.78 | -7.35 | -12.07 | -7.74 | -17.30 | 1.91 |
| | Res-34 | 0.00 | -1.28 | -0.91 | -0.04 | -2.65 | -0.97 | -1.63 | -8.86 | -3.41 | -8.38 | -0.76 | -2.78 | -16.78 | -1.63 |
| | Res-50 | -0.04 | 0.03 | -7.90 | -0.08 | -4.35 | -1.37 | -0.69 | -9.09 | -3.32 | -5.86 | -10.75 | -8.87 | -11.57 | 0.14 |
| | Res-101 | -0.41 | -1.38 | -1.79 | -0.04 | -3.59 | -0.05 | -2.26 | -4.31 | -0.62 | -1.43 | -11.70 | -8.84 | -3.65 | -0.11 |
| BezierLaneNet [4] | Res-18 | 1.53 | -1.74 | -6.62 | 0.51 | -8.70 | -5.68 | -7.96 | -9.00 | -11.68 | -8.99 | -11.91 | -7.81 | -15.48 | 3.32 |
| | Res-34 | -0.38 | -0.58 | -3.66 | -0.16 | -4.32 | -0.29 | -5.67 | -2.28 | -12.34 | -3.55 | -10.81 | -2.20 | -2.05 | -0.87 |
| | Res-50 | -0.02 | -0.85 | -0.22 | -0.15 | -6.32 | -2.55 | -0.75 | -5.01 | -13.15 | -2.59 | -5.69 | -0.78 | -4.42 | 0.02 |
| | Res-101 | -0.29 | -1.62 | -7.59 | -0.06 | -8.21 | -3.08 | -3.37 | -10.04 | -0.50 | -3.19 | -7.84 | 0.16 | -15.20 | -0.90 |
| GANet [13] | Res-18 | -3.29 | -2.61 | -5.76 | -5.09 | -14.47 | -6.57 | -9.81 | -22.05 | -16.39 | -17.86 | -8.40 | -13.94 | -28.18 | 6.52 |
| | Res-34 | -2.74 | -1.65 | -0.99 | -5.70 | -4.03 | 0.15 | -3.23 | -22.87 | -5.33 | -5.28 | -8.17 | -5.10 | -24.26 | -3.89 |
| | Res-50 | -3.15 | -1.96 | -1.81 | -0.31 | -0.16 | -3.87 | -9.88 | -20.08 | -6.03 | -15.34 | -4.83 | -4.95 | -4.63 | -2.18 |
| | Res-101 | -2.65 | -0.51 | -3.73 | -5.03 | -3.18 | -6.02 | -1.18 | -6.03 | -4.97 | -13.88 | -3.56 | -3.26 | -9.69 | -5.25 |
| SCNN [8] | VGG | 7.74 | -4.74 | -3.06 | -5.41 | -8.06 | -5.08 | -7.24 | -17.62 | -14.62 | -14.14 | -13.57 | -10.09 | -16.50 | -6.73 |

Table 4: The breakdown Accuracy results of each illusion type under original scenes and perturbed scenes (%).

(a) Results under original scenes (%).

| Method | Backbone | Road Damage | | | | Traffic Obstruction | | | Shadow | | | | Reflection | | |
|-------------------|----------|-------------|------------|-----------|-----------|---------------------|---------|------------|--------|-------|-------------|-------|-------------|----------|---------|
| | | RoadCrack | RoadRepair | TireMarks | GuardRail | Vehicle | Bicycle | Pedestrian | Fence | Rail | Streetlight | Wire | Streetlight | Sunlight | Vehicle |
| LaneATT [11] | Res-18 | 76.87 | 82.16 | 85.67 | 64.29 | 72.79 | 77.19 | 77.93 | 79.88 | 85.95 | 85.82 | 90.47 | 78.17 | 79.72 | 80.27 |
| | Res-34 | 78.80 | 83.84 | 86.58 | 64.00 | 75.69 | 78.35 | 79.69 | 79.15 | 86.22 | 89.42 | 92.13 | 79.50 | 80.53 | 80.22 |
| | Res-50 | 81.82 | 83.50 | 89.48 | 67.09 | 78.16 | 78.14 | 82.43 | 80.71 | 86.44 | 88.46 | 93.80 | 78.68 | 82.00 | 83.33 |
| | Res-101 | 80.84 | 85.20 | 91.60 | 68.77 | 81.70 | 77.81 | 82.37 | 82.96 | 89.45 | 90.31 | 93.66 | 78.57 | 85.85 | 84.30 |
| UFLD [9] | Res-18 | 73.50 | 70.13 | 69.42 | 64.29 | 70.93 | 67.82 | 63.58 | 71.83 | 77.14 | 70.06 | 77.56 | 69.99 | 73.20 | 69.84 |
| | Res-34 | 73.83 | 73.25 | 72.98 | 68.22 | 71.14 | 66.95 | 63.89 | 75.07 | 76.71 | 70.82 | 79.77 | 72.95 | 75.68 | 70.12 |
| | Res-50 | 76.04 | 73.07 | 74.90 | 70.90 | 70.89 | 68.95 | 65.66 | 76.11 | 79.44 | 70.10 | 81.51 | 75.97 | 74.92 | 71.18 |
| | Res-101 | 78.44 | 73.29 | 75.18 | 74.88 | 74.43 | 71.46 | 66.68 | 76.05 | 79.39 | 71.05 | 80.77 | 75.92 | 77.60 | 74.31 |
| BezierLaneNet [4] | Res-18 | 71.95 | 83.05 | 75.05 | 70.37 | 77.85 | 72.96 | 72.30 | 71.18 | 82.11 | 73.96 | 84.82 | 75.80 | 76.35 | 71.55 |
| | Res-34 | 72.28 | 83.95 | 74.96 | 74.12 | 80.38 | 73.31 | 73.37 | 72.64 | 85.76 | 77.33 | 86.06 | 79.45 | 78.88 | 73.10 |
| | Res-50 | 75.05 | 83.08 | 78.82 | 73.97 | 83.99 | 72.96 | 72.98 | 74.12 | 86.93 | 78.25 | 88.97 | 81.94 | 82.19 | 76.44 |
| | Res-101 | 75.04 | 83.43 | 79.43 | 76.22 | 87.86 | 72.19 | 72.66 | 77.74 | 88.25 | 78.00 | 91.94 | 81.97 | 82.24 | 80.27 |
| GANet [13] | Res-18 | 87.51 | 90.97 | 93.56 | 81.29 | 83.88 | 84.72 | 85.75 | 92.37 | 94.44 | 91.90 | 93.44 | 89.23 | 89.80 | 88.17 |
| | Res-34 | 89.21 | 91.58 | 94.67 | 81.48 | 87.26 | 84.17 | 88.75 | 94.73 | 94.02 | 94.31 | 93.78 | 88.45 | 92.04 | 89.95 |
| | Res-50 | 93.18 | 92.15 | 93.79 | 85.46 | 91.26 | 86.65 | 88.31 | 94.52 | 94.82 | 94.55 | 94.14 | 92.41 | 93.48 | 93.08 |
| | Res-101 | 93.40 | 92.65 | 94.14 | 85.44 | 93.36 | 86.27 | 88.79 | 94.15 | 94.52 | 94.76 | 94.52 | 94.16 | 94.42 | 92.42 |
| SCNN [8] | VGG | 74.51 | 71.22 | 72.49 | 71.29 | 65.55 | 72.43 | 71.56 | 69.27 | 67.35 | 72.73 | 70.89 | 66.61 | 69.42 | 70.82 |

(b) Results under perturbed scenes (%).

| Method | Backbone | Road Damage | | | | Traffic Obstruction | | | Shadow | | | | Reflection | | |
|-------------------|----------|-------------|------------|-----------|-----------|---------------------|---------|------------|--------|-------|-------------|-------|-------------|----------|---------|
| | | RoadCrack | RoadRepair | TireMarks | GuardRail | Vehicle | Bicycle | Pedestrian | Fence | Rail | Streetlight | Wire | Streetlight | Sunlight | Vehicle |
| LaneATT [11] | Res-18 | 75.52 | 80.93 | 82.29 | 63.19 | 70.32 | 74.65 | 74.93 | 74.31 | 80.71 | 77.89 | 85.46 | 73.60 | 67.26 | 81.34 |
| | Res-34 | 78.66 | 82.45 | 83.80 | 63.70 | 73.37 | 76.37 | 79.57 | 77.13 | 85.31 | 87.72 | 87.46 | 74.43 | 79.90 | 80.22 |
| | Res-50 | 81.22 | 82.21 | 87.09 | 66.52 | 75.63 | 77.01 | 79.41 | 76.05 | 83.70 | 85.92 | 89.88 | 73.64 | 79.07 | 83.33 |
| | Res-101 | 80.73 | 84.71 | 89.29 | 68.36 | 80.47 | 76.69 | 79.30 | 79.03 | 89.54 | 87.33 | 93.50 | 75.17 | 82.79 | 84.30 |
| UFLD [9] | Res-18 | 73.02 | 68.23 | 64.53 | 64.06 | 68.33 | 66.16 | 62.11 | 64.71 | 70.39 | 64.35 | 70.70 | 65.11 | 62.46 | 71.86 |
| | Res-34 | 73.36 | 71.11 | 68.86 | 68.21 | 69.36 | 66.79 | 63.46 | 68.79 | 69.23 | 65.75 | 72.16 | 67.40 | 65.77 | 68.92 |
| | Res-50 | 75.49 | 71.51 | 72.28 | 70.84 | 68.59 | 67.08 | 65.02 | 68.15 | 73.21 | 63.58 | 79.01 | 72.13 | 67.38 | 69.84 |
| | Res-101 | 78.19 | 72.85 | 74.76 | 74.82 | 73.59 | 71.26 | 66.40 | 72.89 | 76.36 | 69.59 | 76.99 | 74.42 | 73.70 | 72.62 |
| BezierLaneNet [4] | Res-18 | 71.54 | 79.35 | 72.04 | 68.79 | 73.67 | 71.20 | 69.18 | 56.61 | 74.64 | 67.22 | 76.85 | 71.88 | 66.53 | 72.05 |
| | Res-34 | 72.06 | 83.91 | 72.20 | 73.57 | 77.03 | 73.09 | 70.71 | 67.98 | 77.21 | 70.35 | 83.60 | 74.94 | 78.66 | 72.67 |
| | Res-50 | 74.67 | 81.56 | 75.49 | 73.18 | 79.40 | 71.89 | 71.02 | 65.11 | 81.78 | 73.41 | 85.46 | 79.62 | 79.48 | 75.98 |
| | Res-101 | 74.95 | 79.78 | 77.50 | 75.32 | 87.07 | 70.71 | 70.90 | 66.24 | 86.02 | 75.86 | 90.14 | 79.92 | 79.42 | 80.17 |
| GANet [13] | Res-18 | 85.13 | 88.23 | 88.35 | 78.19 | 77.82 | 82.36 | 81.76 | 77.57 | 87.28 | 80.92 | 87.48 | 81.61 | 74.73 | 90.72 |
| | Res-34 | 88.80 | 89.25 | 94.14 | 78.37 | 86.05 | 84.11 | 88.13 | 81.96 | 90.45 | 94.18 | 87.55 | 79.74 | 91.66 | 88.37 |
| | Res-50 | 91.98 | 90.15 | 88.86 | 83.69 | 88.06 | 86.05 | 83.71 | 84.56 | 94.79 | 94.47 | 94.11 | 90.83 | 81.63 | 91.41 |
| | Res-101 | 92.84 | 91.41 | 91.93 | 85.46 | 92.28 | 83.80 | 86.51 | 91.51 | 94.27 | 93.94 | 92.34 | 91.80 | 92.24 | 90.58 |
| SCNN [8] | VGG | 71.41 | 71.21 | 71.95 | 69.76 | 62.41 | 70.74 | 68.95 | 64.54 | 62.80 | 67.04 | 68.50 | 63.74 | 62.77 | 69.90 |

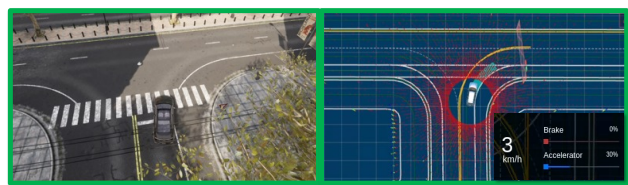
Table 5: The breakdown F1-score results of each illusion type under original scenes and perturbed scenes (%).

(a) Results under original scenes (%).

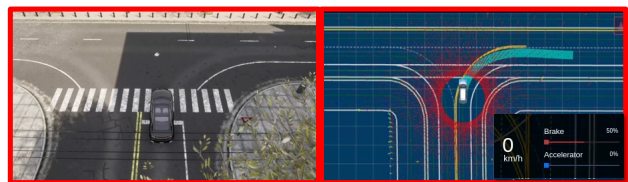
| Method | Backbone | Road Damage | | | | Traffic Obstruction | | | Shadow | | | | Reflection | | |
|-------------------|----------|-------------|------------|-----------|-----------|---------------------|---------|------------|--------|-------|-------------|-------|-------------|----------|---------|
| | | RoadCrack | RoadRepair | TireMarks | GuardRail | Vehicle | Bicycle | Pedestrian | Fence | Rail | Streetlight | Wire | Streetlight | Sunlight | Vehicle |
| LaneATT [11] | Res-18 | 42.46 | 58.58 | 68.33 | 23.58 | 45.64 | 57.02 | 53.73 | 47.11 | 62.13 | 55.23 | 74.15 | 53.16 | 54.14 | 51.78 |
| | Res-34 | 44.24 | 59.23 | 70.12 | 22.96 | 49.24 | 58.43 | 56.95 | 50.66 | 63.67 | 58.49 | 76.14 | 55.12 | 55.09 | 52.60 |
| | Res-50 | 46.14 | 61.40 | 70.31 | 23.66 | 48.77 | 61.02 | 59.64 | 50.50 | 67.33 | 58.93 | 78.82 | 56.52 | 58.40 | 51.98 |
| | Res-101 | 46.88 | 62.67 | 72.93 | 26.48 | 51.23 | 60.84 | 61.46 | 52.87 | 71.14 | 59.20 | 81.50 | 56.92 | 59.26 | 53.39 |
| UFLD [9] | Res-18 | 36.44 | 28.67 | 29.00 | 10.91 | 36.48 | 31.18 | 27.33 | 27.25 | 43.04 | 28.39 | 45.89 | 28.84 | 33.37 | 33.41 |
| | Res-34 | 39.31 | 28.25 | 30.03 | 10.75 | 39.75 | 33.51 | 27.26 | 29.63 | 46.08 | 30.33 | 46.86 | 28.21 | 34.57 | 37.12 |
| | Res-50 | 42.02 | 30.02 | 29.29 | 13.12 | 42.79 | 35.59 | 29.30 | 31.68 | 46.25 | 32.82 | 48.84 | 31.20 | 36.27 | 37.57 |
| | Res-101 | 41.64 | 32.43 | 28.98 | 15.22 | 42.95 | 35.57 | 31.30 | 35.30 | 49.79 | 32.77 | 49.40 | 32.14 | 39.54 | 41.39 |
| BezierLaneNet [4] | Res-18 | 34.41 | 59.18 | 41.02 | 22.91 | 59.23 | 44.03 | 45.66 | 38.41 | 63.04 | 35.94 | 66.82 | 47.78 | 50.17 | 30.76 |
| | Res-34 | 35.08 | 58.52 | 40.97 | 25.73 | 62.63 | 44.55 | 48.57 | 40.63 | 66.87 | 35.00 | 66.36 | 49.14 | 50.39 | 33.58 |
| | Res-50 | 36.27 | 62.28 | 42.00 | 25.69 | 62.88 | 44.36 | 47.78 | 44.11 | 70.26 | 36.73 | 68.55 | 48.53 | 52.78 | 36.52 |
| | Res-101 | 37.97 | 64.68 | 44.21 | 28.39 | 63.54 | 46.50 | 47.86 | 44.10 | 70.51 | 40.55 | 71.43 | 48.71 | 56.04 | 37.37 |
| GANet [13] | Res-18 | 84.23 | 86.93 | 94.69 | 64.51 | 83.31 | 79.87 | 78.87 | 87.13 | 93.75 | 84.32 | 92.99 | 81.87 | 86.90 | 80.18 |
| | Res-34 | 87.43 | 90.19 | 94.85 | 67.59 | 86.76 | 83.37 | 80.49 | 90.59 | 94.99 | 83.34 | 94.76 | 82.91 | 90.80 | 79.58 |
| | Res-50 | 87.25 | 89.26 | 95.21 | 67.77 | 88.73 | 87.23 | 83.60 | 90.76 | 95.48 | 85.48 | 95.33 | 83.14 | 91.15 | 83.25 |
| | Res-101 | 88.23 | 90.98 | 95.33 | 67.01 | 89.77 | 87.20 | 86.68 | 91.50 | 95.82 | 87.67 | 95.28 | 85.52 | 92.88 | 85.91 |
| SCNN [8] | VGG | 56.81 | 37.94 | 63.96 | 49.31 | 42.30 | 55.86 | 54.29 | 54.08 | 46.16 | 48.34 | 51.91 | 40.69 | 51.76 | 61.19 |

(b) Results under perturbed scenes (%).

| Method | Backbone | Road Damage | | | | Traffic Obstruction | | | Shadow | | | | Reflection | | |
|-------------------|----------|-------------|------------|-----------|-----------|---------------------|---------|------------|--------|-------|-------------|-------|-------------|----------|---------|
| | | RoadCrack | RoadRepair | TireMarks | GuardRail | Vehicle | Bicycle | Pedestrian | Fence | Rail | Streetlight | Wire | Streetlight | Sunlight | Vehicle |
| LaneATT [11] | Res-18 | 38.64 | 55.14 | 65.02 | 23.22 | 39.68 | 52.15 | 47.06 | 41.63 | 48.29 | 39.95 | 63.41 | 46.21 | 28.53 | 54.93 |
| | Res-34 | 40.40 | 56.20 | 68.27 | 22.84 | 46.18 | 58.10 | 51.44 | 46.58 | 61.67 | 54.95 | 71.10 | 54.83 | 44.95 | 52.60 |
| | Res-50 | 44.91 | 61.38 | 67.61 | 23.49 | 46.91 | 55.86 | 55.80 | 46.78 | 61.14 | 48.84 | 69.95 | 50.51 | 43.62 | 51.95 |
| | Res-101 | 43.64 | 61.36 | 70.45 | 26.21 | 48.92 | 56.90 | 61.18 | 48.00 | 61.53 | 55.21 | 73.89 | 56.55 | 46.97 | 53.36 |
| UFLD [9] | Res-18 | 37.60 | 27.47 | 22.00 | 10.70 | 31.47 | 28.12 | 24.69 | 18.98 | 30.27 | 21.03 | 33.81 | 21.10 | 16.07 | 35.31 |
| | Res-34 | 38.95 | 27.31 | 25.81 | 10.52 | 35.32 | 31.68 | 25.43 | 23.47 | 41.42 | 21.77 | 40.60 | 22.58 | 21.16 | 36.93 |
| | Res-50 | 41.58 | 29.82 | 23.81 | 13.02 | 38.57 | 35.15 | 27.13 | 27.31 | 37.27 | 32.36 | 40.36 | 28.25 | 22.69 | 37.18 |
| | Res-101 | 41.45 | 32.39 | 20.89 | 15.18 | 39.82 | 34.67 | 28.66 | 26.35 | 42.86 | 28.45 | 49.16 | 26.26 | 20.10 | 40.02 |
| BezierLaneNet [4] | Res-18 | 35.94 | 57.44 | 34.39 | 23.43 | 50.53 | 38.36 | 37.70 | 29.41 | 51.36 | 26.95 | 54.91 | 39.96 | 34.68 | 34.07 |
| | Res-34 | 34.88 | 58.02 | 37.89 | 25.76 | 58.60 | 40.85 | 45.03 | 33.38 | 64.62 | 31.33 | 54.10 | 41.75 | 49.32 | 31.14 |
| | Res-50 | 35.89 | 62.14 | 35.78 | 25.68 | 57.44 | 40.88 | 44.73 | 38.59 | 68.49 | 35.73 | 58.17 | 41.04 | 47.45 | 33.99 |
| | Res-101 | 37.93 | 62.86 | 39.06 | 28.31 | 58.14 | 45.99 | 46.68 | 35.37 | 58.77 | 30.86 | 67.69 | 44.20 | 40.05 | 37.42 |
| GANet [13] | Res-18 | 80.94 | 84.32 | 88.93 | 59.41 | 68.84 | 73.30 | 69.07 | 65.08 | 77.35 | 66.46 | 84.59 | 67.94 | 58.72 | 86.69 |
| | Res-34 | 85.11 | 87.97 | 94.49 | 64.90 | 72.04 | 83.39 | 77.86 | 79.03 | 83.35 | 68.99 | 92.52 | 72.79 | 67.13 | 74.26 |
| | Res-50 | 86.01 | 86.96 | 94.93 | 66.80 | 79.62 | 79.84 | 75.06 | 66.35 | 81.72 | 83.26 | 92.13 | 76.66 | 83.84 | 82.64 |
| | Res-101 | 85.15 | 88.97 | 96.40 | 63.95 | 79.24 | 85.52 | 85.60 | 78.79 | 84.87 | 84.20 | 87.49 | 77.11 | 67.04 | 85.54 |
| SCNN [8] | VGG | 64.55 | 33.20 | 60.90 | 43.90 | 34.24 | 50.77 | 47.05 | 36.45 | 31.54 | 34.20 | 38.33 | 30.60 | 35.26 | 54.46 |



(a) original scenario



(b) perturbed scenario

Figure 3: The shadow case causes Apollo to make incorrect decisions.

REFERENCES

- [1] Mohamed Aly. 2008. Real time detection of lane markers in urban streets. In *IV*.
- [2] Karsten Behrendt and Ryan Soussan. 2019. Unsupervised labeled lane markers using maps. In *ICCV Workshop*.
- [3] Terrance DeVries and Graham W Taylor. 2017. Improved regularization of convolutional neural networks with cutout. *arXiv preprint arXiv:1708.04552* (2017).
- [4] Zhengyang Feng, Shaohua Guo, Xin Tan, Ke Xu, Min Wang, and Lizhuang Ma. 2022. Rethinking efficient lane detection via curve modeling. In *CVPR*.
- [5] Golnaz Ghiasi, Yin Cui, Aravind Srinivas, Rui Qian, Tsung-Yi Lin, Ekin D Cubuk, Quoc V Le, and Barret Zoph. 2021. Simple copy-paste is a strong data augmentation method for instance segmentation. In *CVPR*.
- [6] Seokju Lee, Junsik Kim, Jae Shin Yoon, Seunghak Shin, Oleksandr Bailo, Namil Kim, Tae-Hee Lee, Hyun Seok Hong, Seung-Hoon Han, and In So Kweon. 2017. Vpnet: Vanishing point guided network for lane and road marking detection and recognition. In *ICCV*.
- [7] Aleksander Madry, Aleksandar Makelov, Ludwig Schmidt, Dimitris Tsipras, and Adrian Vladu. 2017. Towards deep learning models resistant to adversarial attacks. *arXiv preprint arXiv:1706.06083* (2017).
- [8] Xingang Pan, Jianping Shi, Ping Luo, Xiaogang Wang, and Xiaoou Tang. 2018. Spatial as deep: Spatial cnn for traffic scene understanding. In *AAAI*.
- [9] Zequn Qin, HuanYu Wang, and Xi Li. 2020. Ultra fast structure-aware deep lane detection. In *ECCV*.
- [10] Takami Sato, Junjie Shen, Ningfei Wang, Yunhan Jia, Xue Lin, and Qi Alfred Chen. 2021. Dirty road can attack: Security of deep learning based automated lane centering under {Physical-World} attack. In *USENIX Security*.
- [11] Lucas Tabelini, Rodrigo Berriel, Thiago M Paixao, Claudine Badue, Alberto F De Souza, and Thiago Oliveira-Santos. 2021. Keep your eyes on the lane: Real-time attention-guided lane detection. In *CVPR*.
- [12] Tusimple. 2017. Tusimple Benchmark. <https://github.com/TuSimple/tusimple-benchmark>.
- [13] Jinsheng Wang, Yinchao Ma, Shaofei Huang, Tianrui Hui, Fei Wang, Chen Qian, and Tianzhu Zhang. 2022. A keypoint-based global association network for lane detection. In *CVPR*.
- [14] Hang Xu, Shaoju Wang, Xinyue Cai, Wei Zhang, Xiaodan Liang, and Zhenguo Li. 2020. Curvelane-nas: Unifying lane-sensitive architecture search and adaptive point blending. In *ECCV*.
- [15] Fisher Yu, Haofeng Chen, Xin Wang, Wenqi Xian, Yingying Chen, Fangchen Liu, Vashisht Madhavan, and Trevor Darrell. 2020. Bdd100k: A diverse driving dataset for heterogeneous multitask learning. In *CVPR*.
- [16] Yujun Zhang, Lei Zhu, Wei Feng, Huazhu Fu, Mingqian Wang, Qingxia Li, Cheng Li, and Song Wang. 2021. Vil-100: A new dataset and a baseline model for video instance lane detection. In *ICCV*.